A THERMAL RADIANCE MODEL FOR THE MOON AND MERCURY

Kay Wohlfarth, Christian Wöhler

technische universität dortmund

A&A 674, A69 (2023)
https://doi.org/10.1051/0004-6361/202245343

Astronomy & Astrophysics

An advanced thermal roughness model for airless planetary bodies

Implications for global variations of lunar hydration and mineralogical mapping of Mercury with the MERTIS spectrometer★

Kay Wohlfarth[1], Christian Wöhler[1], Harald Hiesinger[2], and Jörn Helbert[3]

[1] Image Analysis Group, TU Dortmund University, Otto-Hahn-Str. 4, 44227 Dortmund, Germany
e-mail: kay.wohlfarth@tu-dortmund.de
[2] Institute for Planetology, Wilhelm-Klemm-Str. 10, 48149 Münster, Germany
[3] Institute for Planetary Research, DLR, Rutherfordstr. 2, 12489 Berlin, Germany

Received 31 October 2022 / Accepted 22 March 2023

ABSTRACT

We present a combined reflectance and thermal radiance model for airless planetary bodies. The Hapke model provides the reflected component. The developed thermal model is the first to consistently use rough fractal surfaces, self-scattering, self-heating, and disk-resolved bolometric albedo for entire planets. We validated the model with disk-resolved lunar measurements acquired by the Chinese weather satellite Gaofen-4 at around 3.5–4.1 µm and measurements of the Diviner lunar radiometer at 8.25 µm and 25–41 µm, finding nearly exact agreement. Further, we reprocessed the thermal correction of the global lunar reflectance maps obtained by the Moon Mineralogy Mapper M^3 and employed the new model to correct excess thermal radiance. The results confirm the diurnal, latitudinal, and compositional variations of lunar hydration reported in previous and recent studies with other instruments. Further, we compared the model to lunar measurements obtained by the Mercury Radiometer and Thermal Infrared Spectrometer (MERTIS) on board BepiColombo during a flyby maneuver on April 9, 2020: the measured and the modeled radiance variations across the disk match. Finally, we adapted the thermal model to Mercury for emissivity calibration of upcoming Mercury flyby measurements and in-orbit operation. Although a physical parameter must be invariant under various observation scenarios, the best lunar surface roughness fits vary between different datasets. We critically discuss possible reasons and conclude that anisotropic emissivity modeling has room for improvement and requires attention in future studies.

Key words. Moon – infrared: planetary systems – radiation mechanisms: thermal – methods: data analysis – methods: numerical – planets and satellites: surfaces

Today

- Thermal model basics
- New: accuracy analysis
- New: comparison with more datasets
- Outlook

Wohlfarth et al. 2023

Thermal Model 1/2

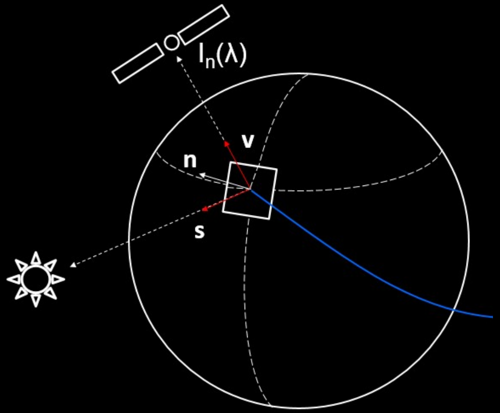

Geometry

- Sub-solar point
- Sub-spacecraft point
- Solar distance
- Observer distance

Wohlfarth et al. 2023

Thermal Model 1/2

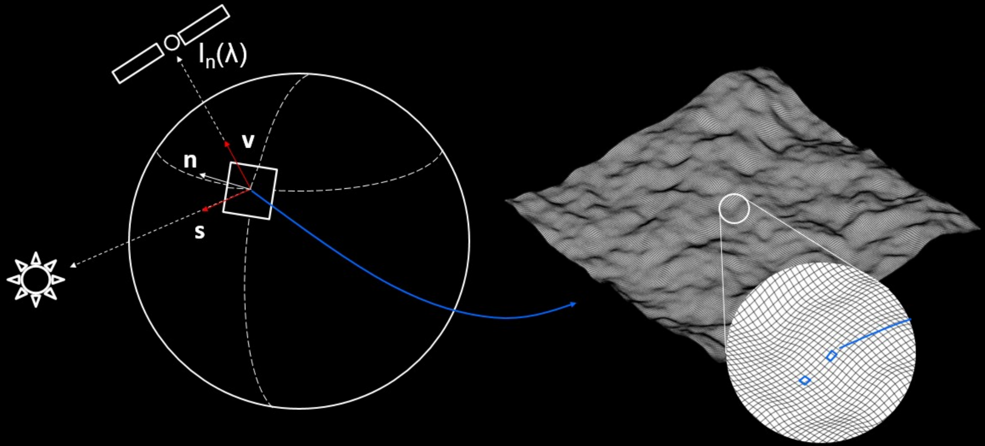

Geometry

- Sub-solar point
- Sub-spacecraft point
- Solar distance
- Observer distance

Surface

- Fractal Roughness $\bar{\theta} = 30°$
- Emissivity $\varepsilon(\lambda, e)$

Wohlfarth et al. 2023

Thermal Model 1/2

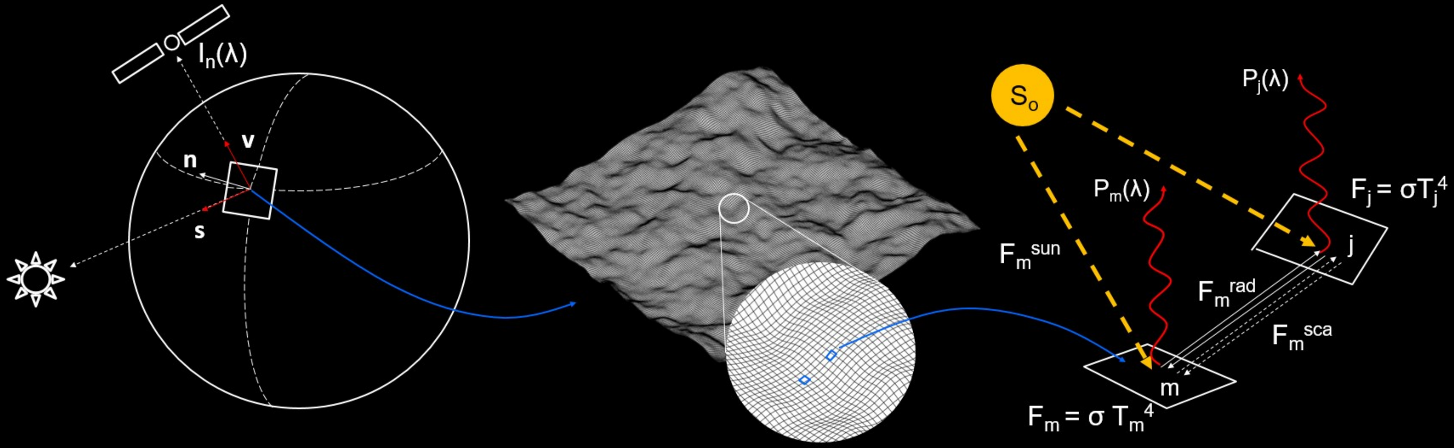

Geometry

- Sub-solar point
- Sub-spacecraft point
- Solar distance
- Observer distance

Surface

- Fractal Roughness $\bar{\theta} = 30°$
- Emissivity $\varepsilon(\lambda, e)$

Model

- Self-scattering
- Self-heating
- Efficient linear algebra → fast

Wohlfarth et al. 2023

Thermal Model 1/2

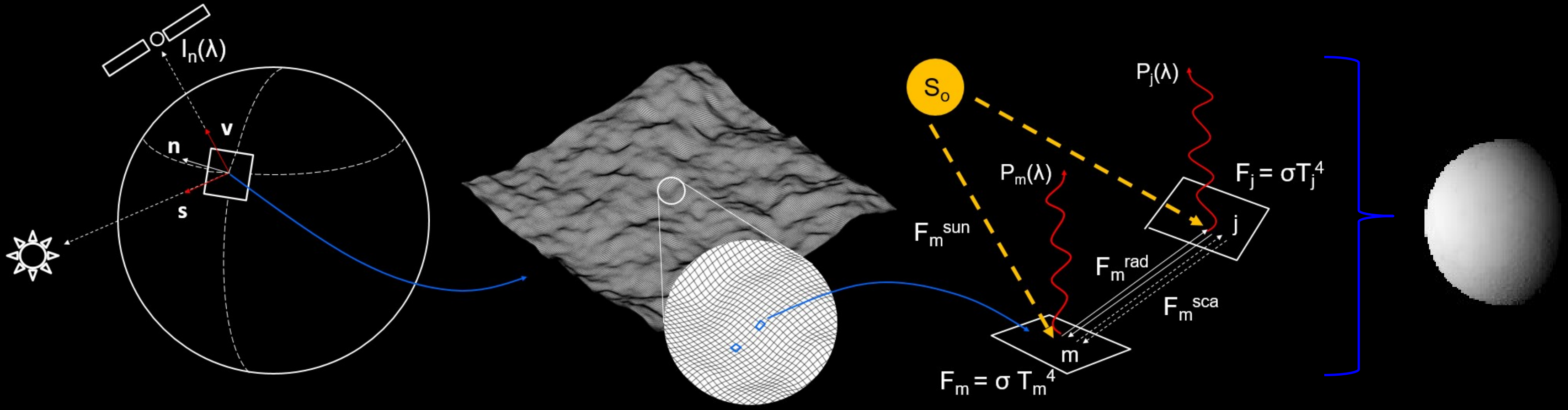

Geometry
- Sub-solar point
- Sub-spacecraft point
- Solar distance
- Observer distance

Surface
- Fractal Roughness $\bar{\theta} = 30°$
- Emissivity $\varepsilon(\lambda, e)$

Model
- Self-scattering
- Self-heating
- Efficient linear algebra → fast

Result
- Disk-resolved
- Projected
- Radiance [W/m²/µm/sr]

Thermal model 2/2

$\phi = 0°$

$\phi = 180°$

Disk-integrated simulations

Consider the „usual suspects“

- Point/line spread function
- Spectral response
- Solid angle per pixel

Datasets

1. Gaofen-4	resolved, 4.8µm	Wu et al. 2021
2. Diviner LRO	tracks, 8.25 µm, 25-41 µm	Bandfield et al. 2015

Datasets

1. Gaofen-4	resolved, 4.8µm	Wu et al. 2021
2. Diviner LROC	tracks, 8.25 µm, 25-41 µm	Bandfield et al. 2015
3. HIRS-2/3/4 NOAA, MetOp	inegrated, 19 ch, 3-13 µm	Müller et al. 2021
4. FOREST-2	resolved, 3.8; 8.8; 11.4 µm	Ororatech

Datasets

1. Gaofen-4	resolved, 4.8µm	Wu et al. 2021
2. Diviner LROC	tracks, 8.25 µm, 25-41 µm	Bandfield et al. 2015
3. HIRS-2/3/4 NOAA, MetOp	inegrated, 19 ch, 3-13 µm	Müller et al. 2021
4. FOREST-2	resolved, 3.8; 8.8; 11.4 µm	Ororatech
5. MODIS Aqua, Terra	resolved, 6 ch, 3.6-12.3 µm	
6. VIIRS J1, J2, NPP	resolved, 5 ch, 3.6-12.5 µm	
7. SLSTR Sentinel-3 A, B	resolved	

Measurement July 30, 2018 (Wu et al. 2018)

Measurement July 30, 2018 (Wu et al. 2018)

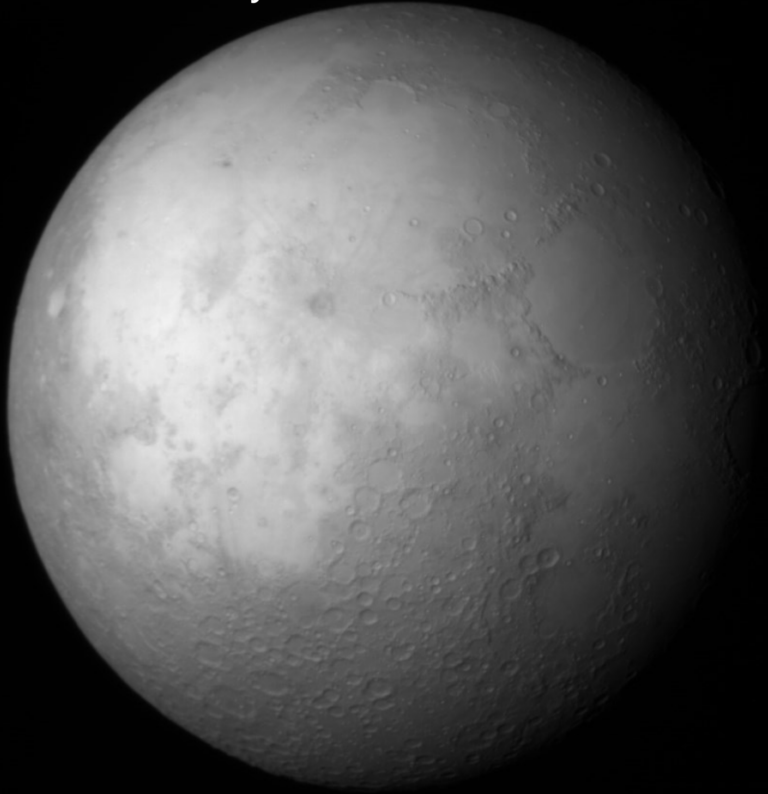

Our model (Wohlfarth et al. 2023)

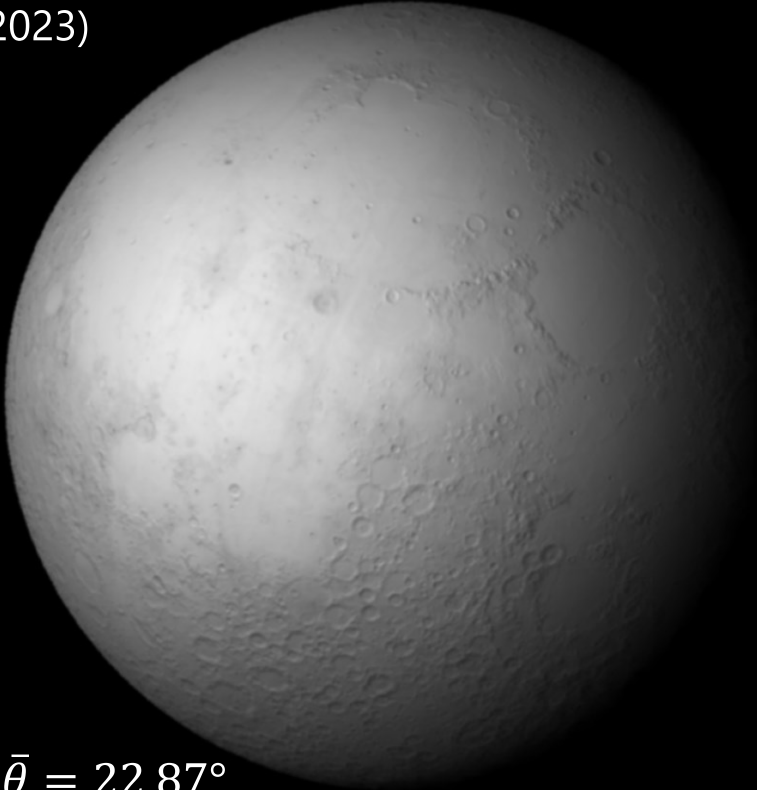

$\bar{\theta} = 22.87°$

RMSE between model and measurement for July 30, 2018

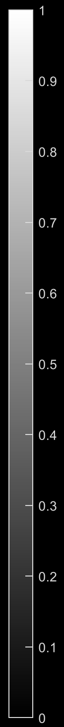

→ Avg. RMSE = 0.2325 W $m^{-2}\mu m^{-1}sr^{-1}$

→ Avg. RMSE/max radiance = 2.91 %

RMSE between model and measurement for July 30, 2018

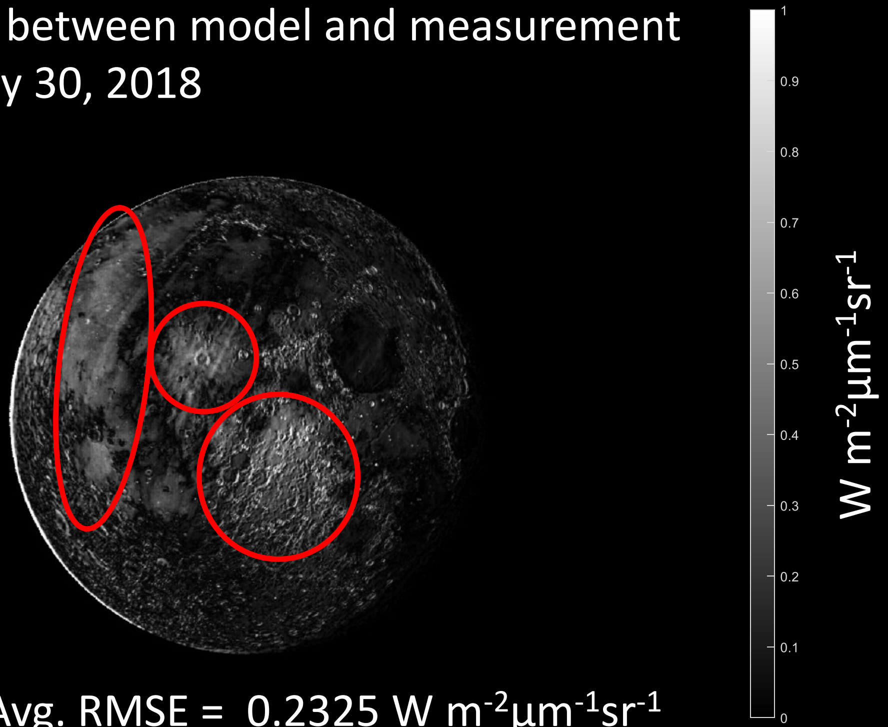

- → Avg. RMSE = 0.2325 $W\ m^{-2}\mu m^{-1}sr^{-1}$
- → Avg. RMSE/max radiance = 2.91 %

RMSE between model and measurement for July 30, 2018

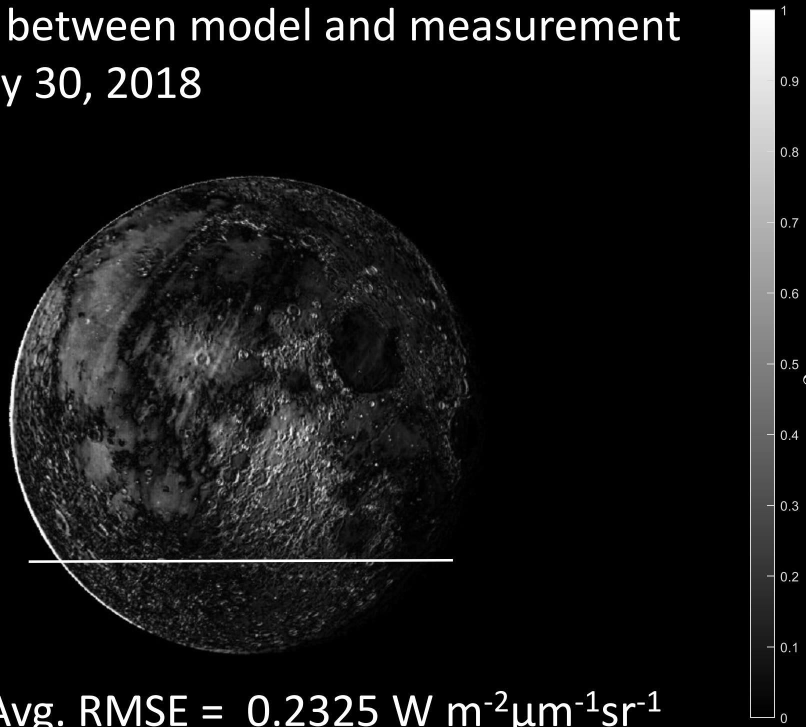

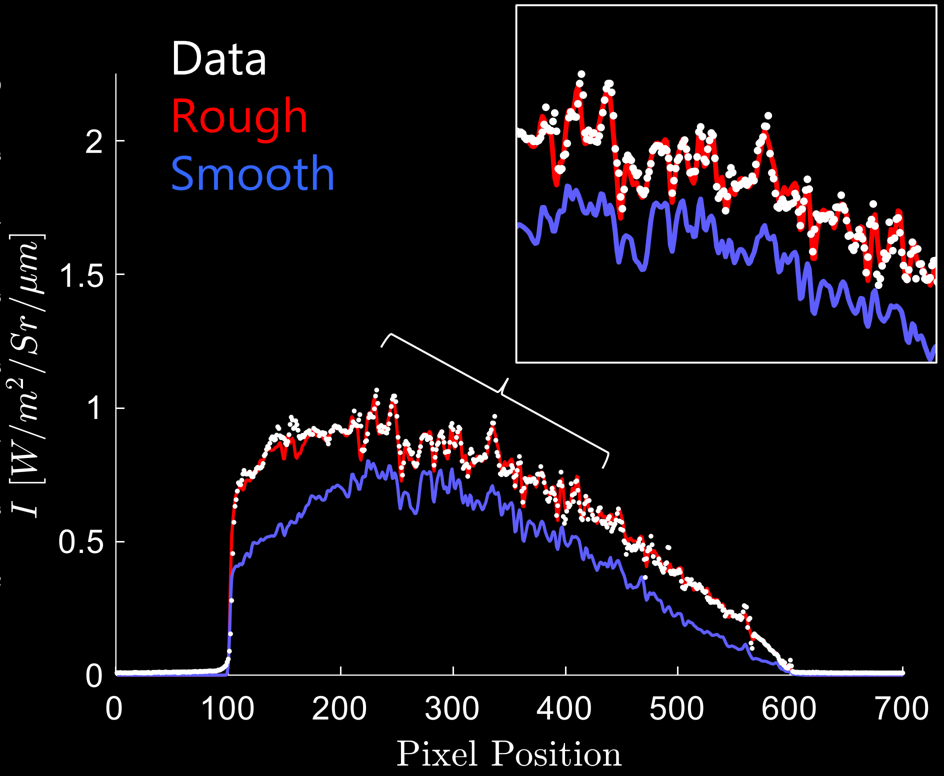

→ Avg. RMSE = 0.2325 W $m^{-2}\mu m^{-1}sr^{-1}$

→ Avg. RMSE/max radiance = 2.91 %

RMSE between model and measurement for July 30, 2018

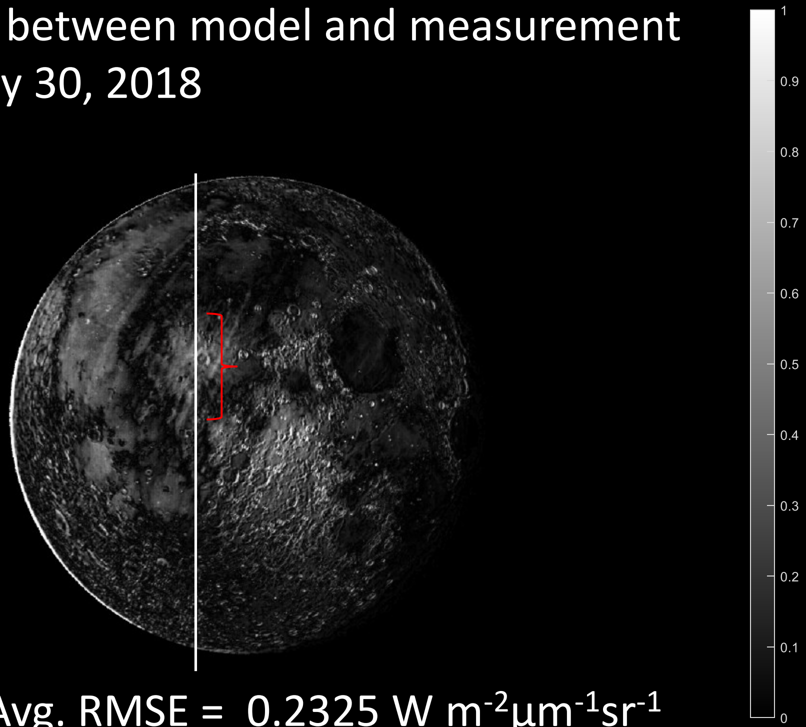

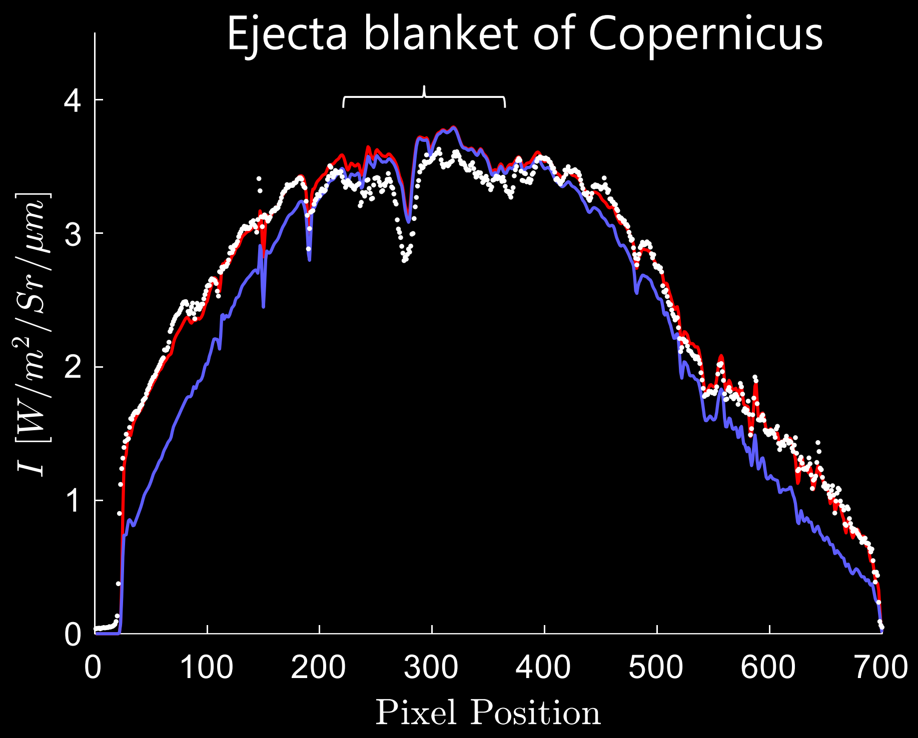

→ Avg. RMSE = 0.2325 W $m^{-2}\mu m^{-1}sr^{-1}$

→ Avg. RMSE/max radiance = 2.91 %

RMSE between model and measurement for July 30, 2018

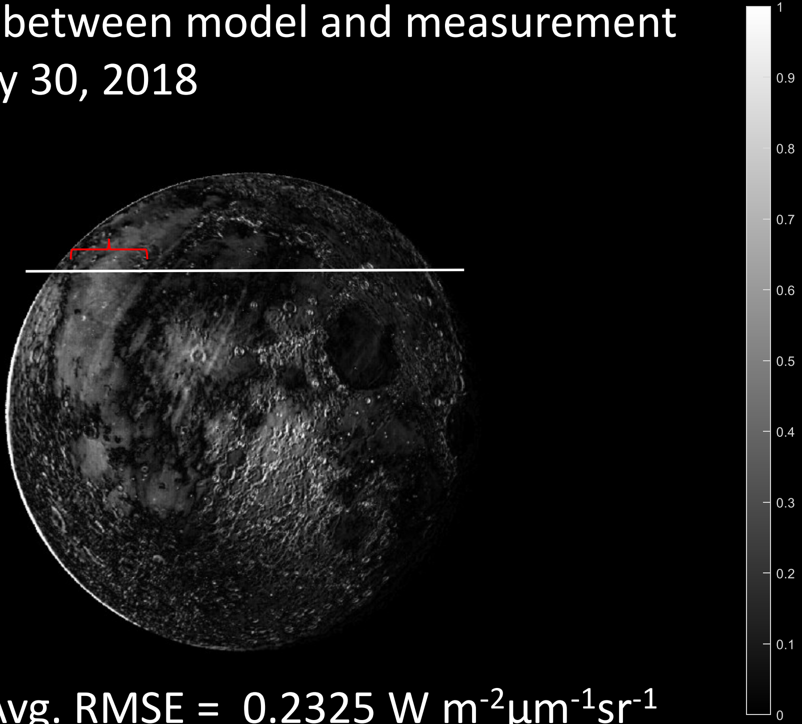

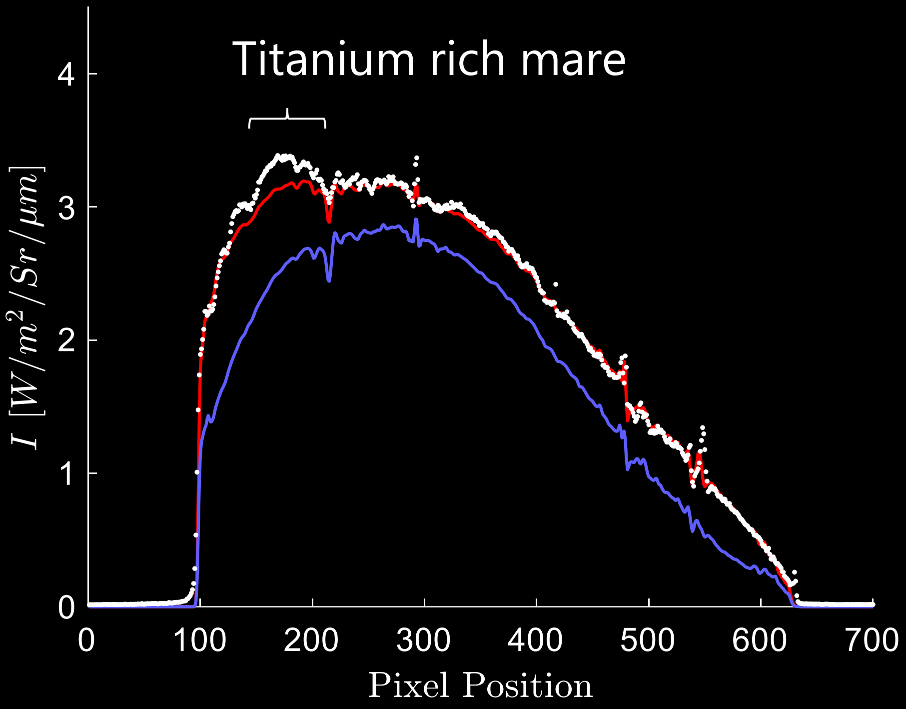

→ Avg. RMSE = 0.2325 W $m^{-2}\mu m^{-1}sr^{-1}$

→ Avg. RMSE/max radiance = 2.91 %

RMSE between model and measurement for July 30, 2018

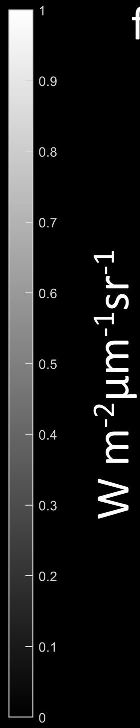

→ Avg. RMSE = 0.2325 W $m^{-2}\mu m^{-1}sr^{-1}$
→ Avg. RMSE/max radiance = 2.91 %

for July 25, 2018

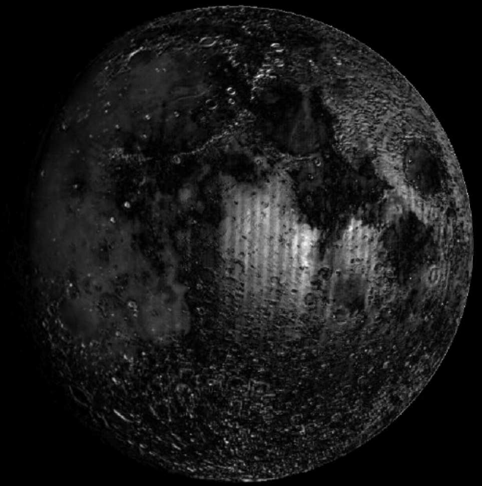

→ Avg. RMSE = 0.1985 W $m^{-2}\mu m^{-1}sr^{-1}$
→ Avg. RMSE/max radiance = 2.48 %

Diviner EPF Measurements

Wohlfarth et al. 2023, EPF positions from Bandfield et al. 2015

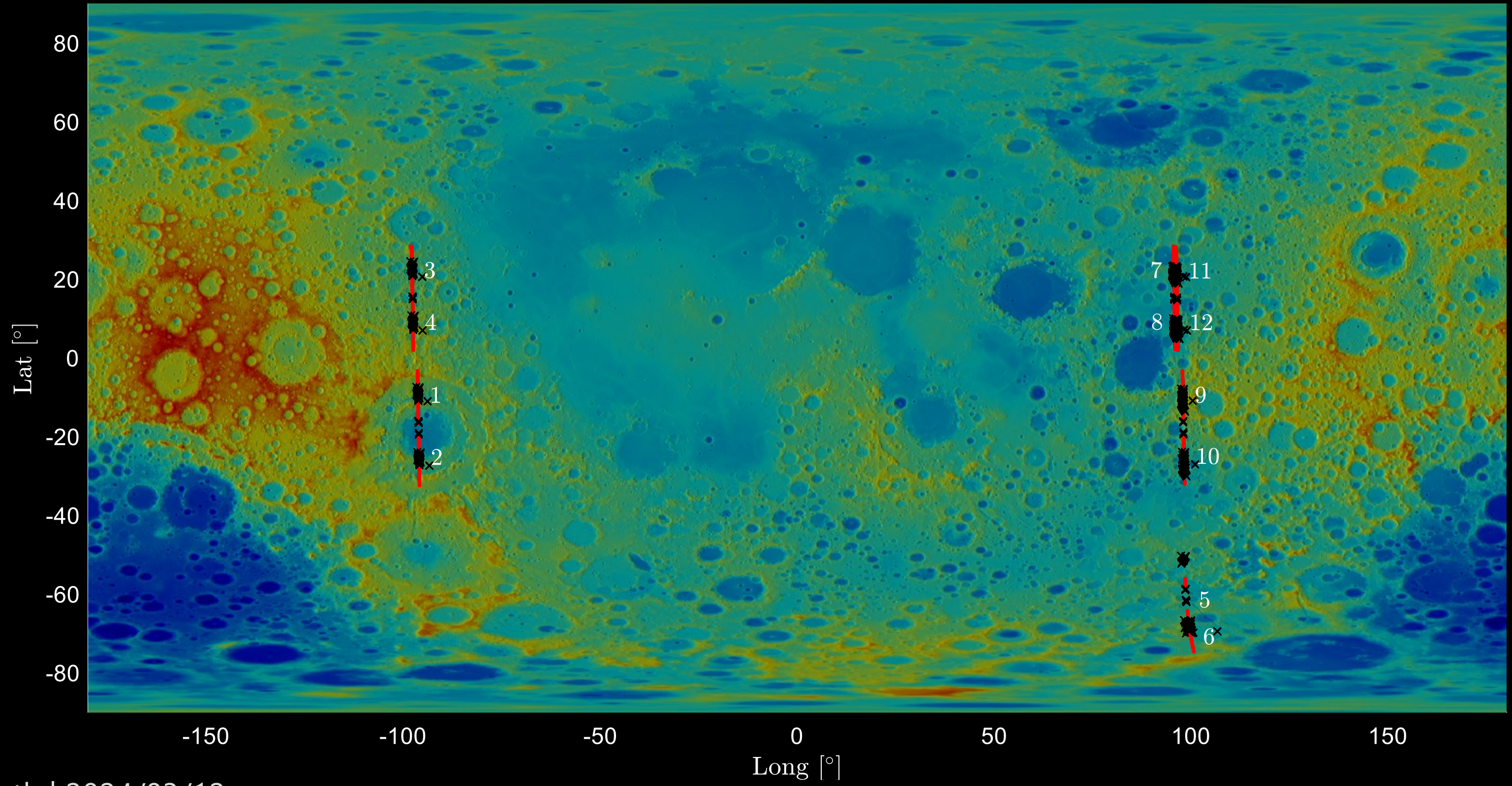

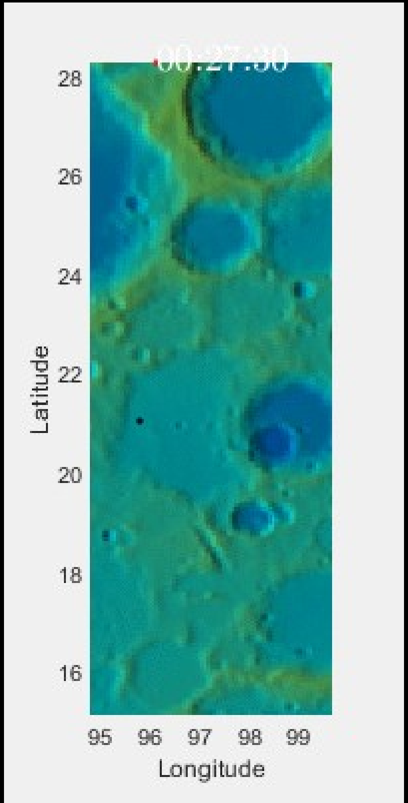
00:27:30
28
26
24
22
20
18
16
Latitude
95
96
97
98
99
Longitude

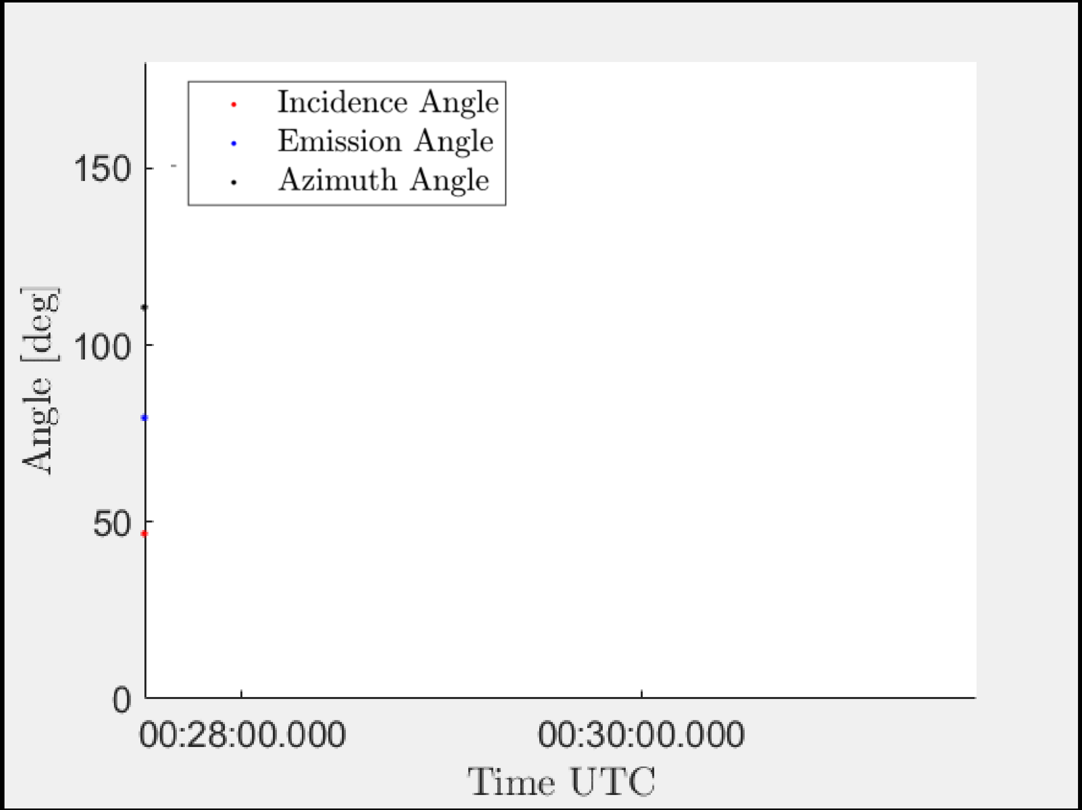
Incidence Angle
Emission Angle
Azimuth Angle
150
100
50
0
Angle [deg]
00:28:00.000
00:30:00.000
Time UTC

Validation with Diviner: EPF

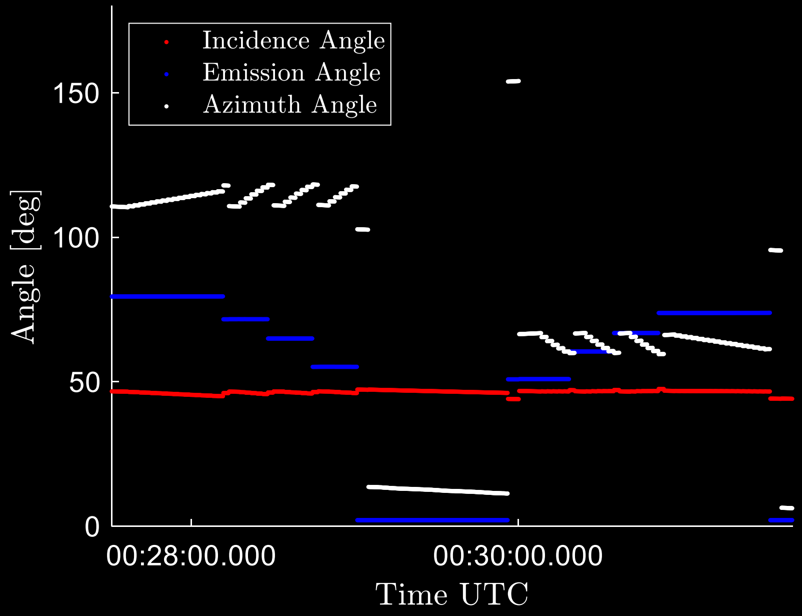

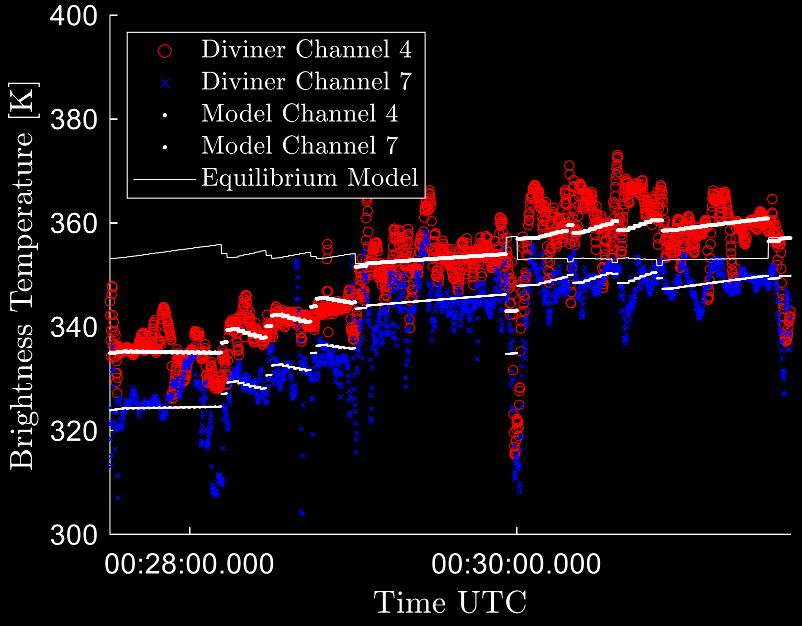

$\bar{\theta} = 28°$

Validation with Diviner: EPF

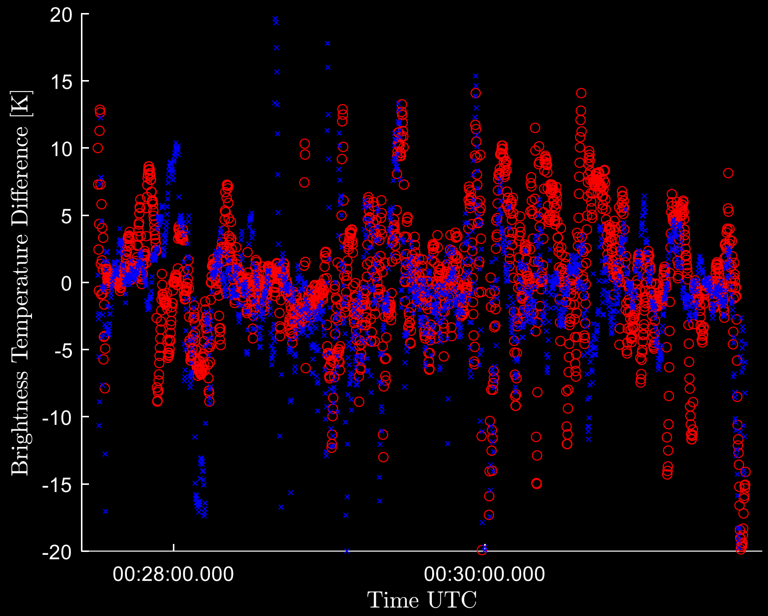

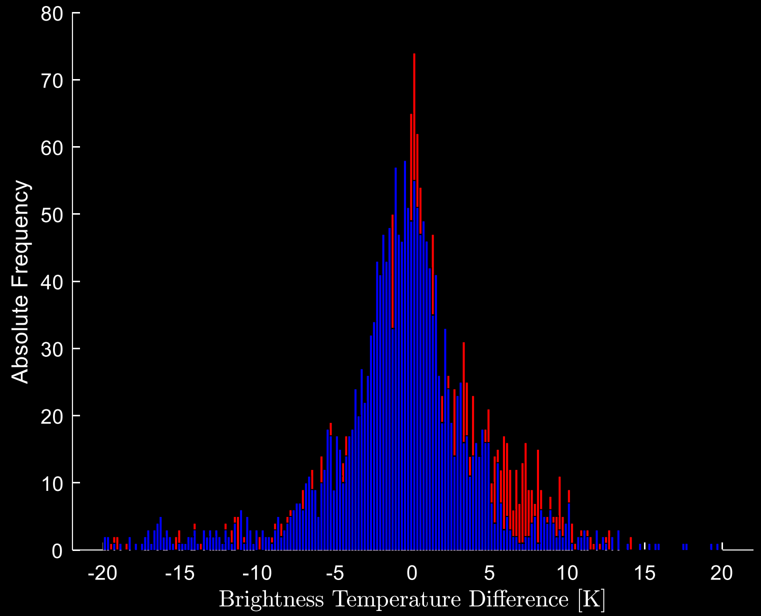

→ RMSE ch. 4 = 5.5982 K

→ RMSE ch. 7 = 6.1130 K

HIRS-2/3/4
Channel 8
11.1 µm

NOAA-11
NOAA-14
NOAA-15
NOAA-17
NOAA-18
NOAA-19
MetOp-A
MetOp-B

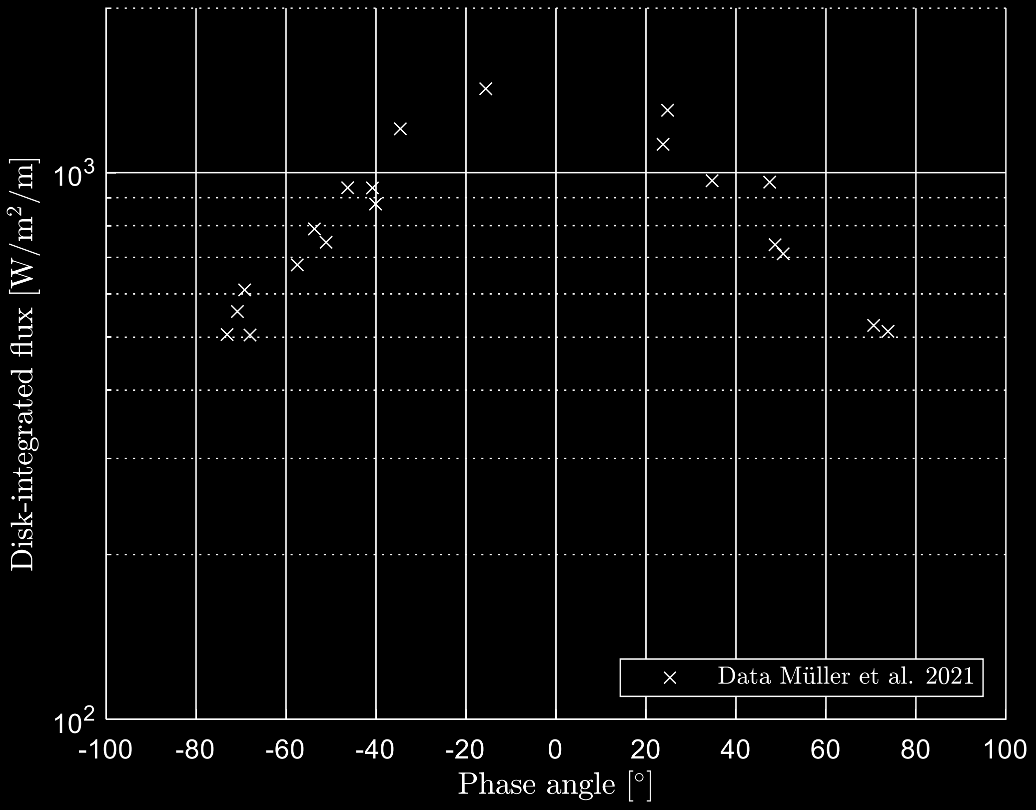

HIRS-2/3/4
Channel 8
11.1 µm

NOAA-11
NOAA-14
NOAA-15
NOAA-17
NOAA-18
NOAA-19
MetOp-A
MetOp-B

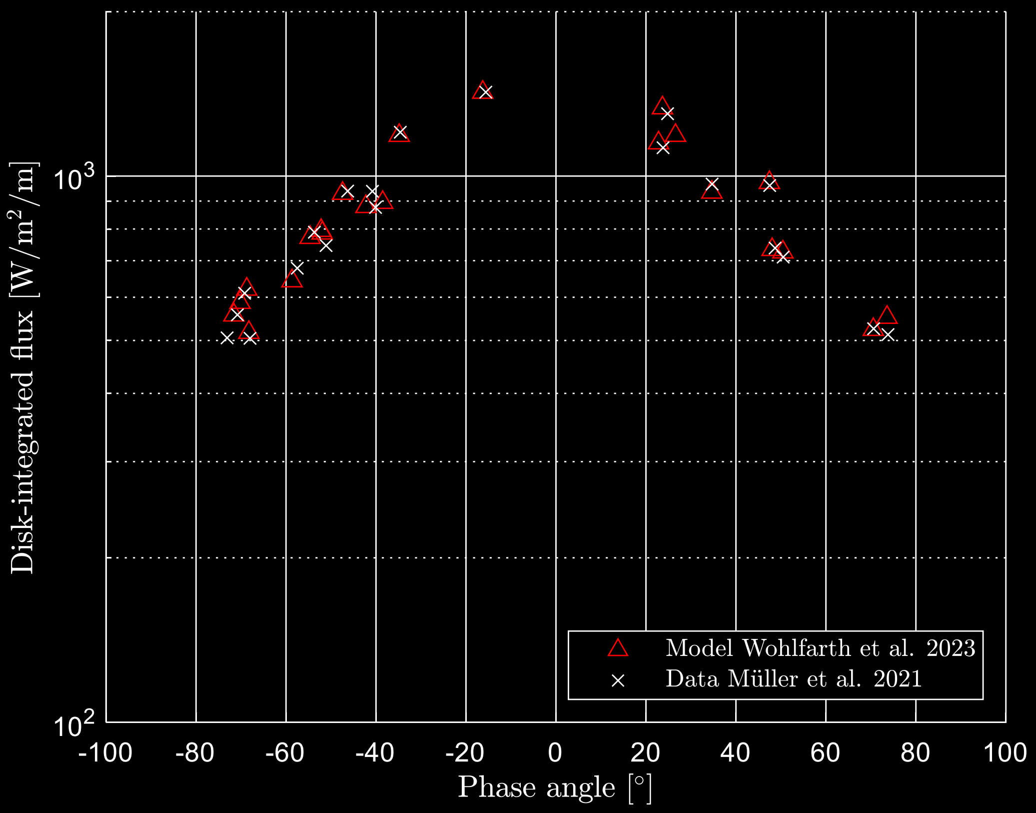

HIRS-2/3/4
Channel 8
11.1 µm

NOAA-11
NOAA-14
NOAA-15
NOAA-17
NOAA-18
NOAA-19
MetOp-A
MetOp-B

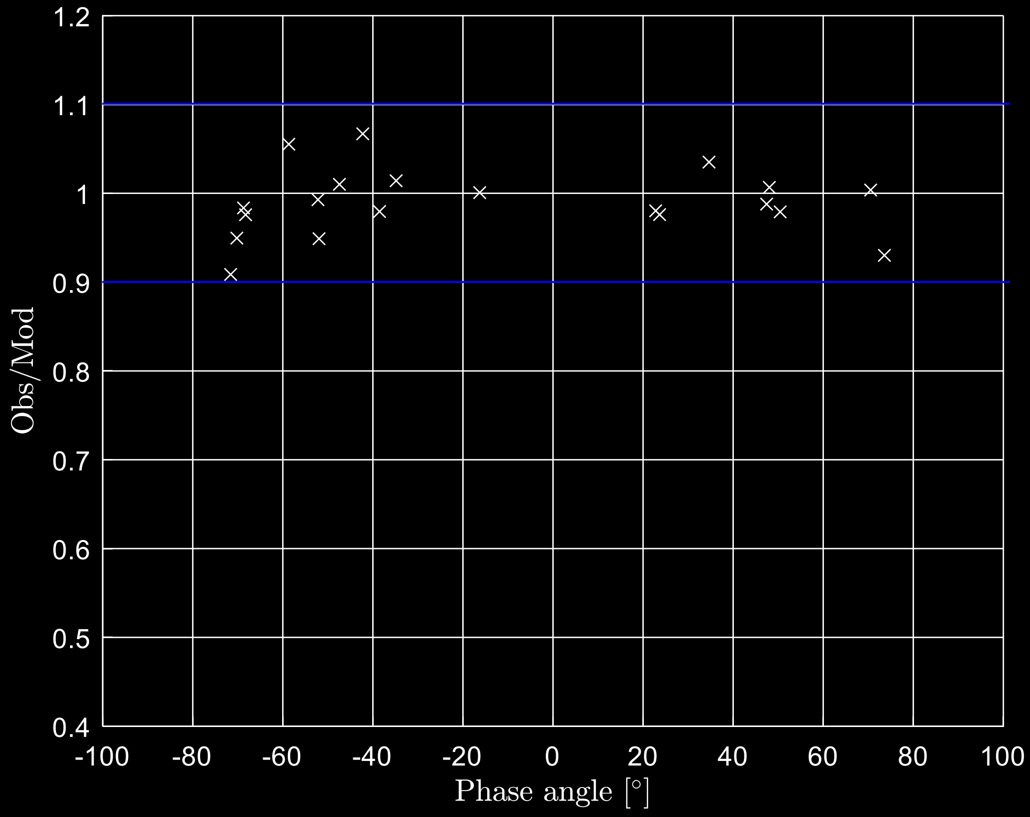

Müller et al. 2021

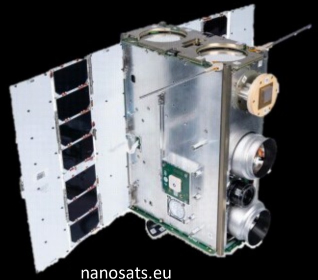

FOREST-2
OroraTech
LWIR band 2
11.4 µm

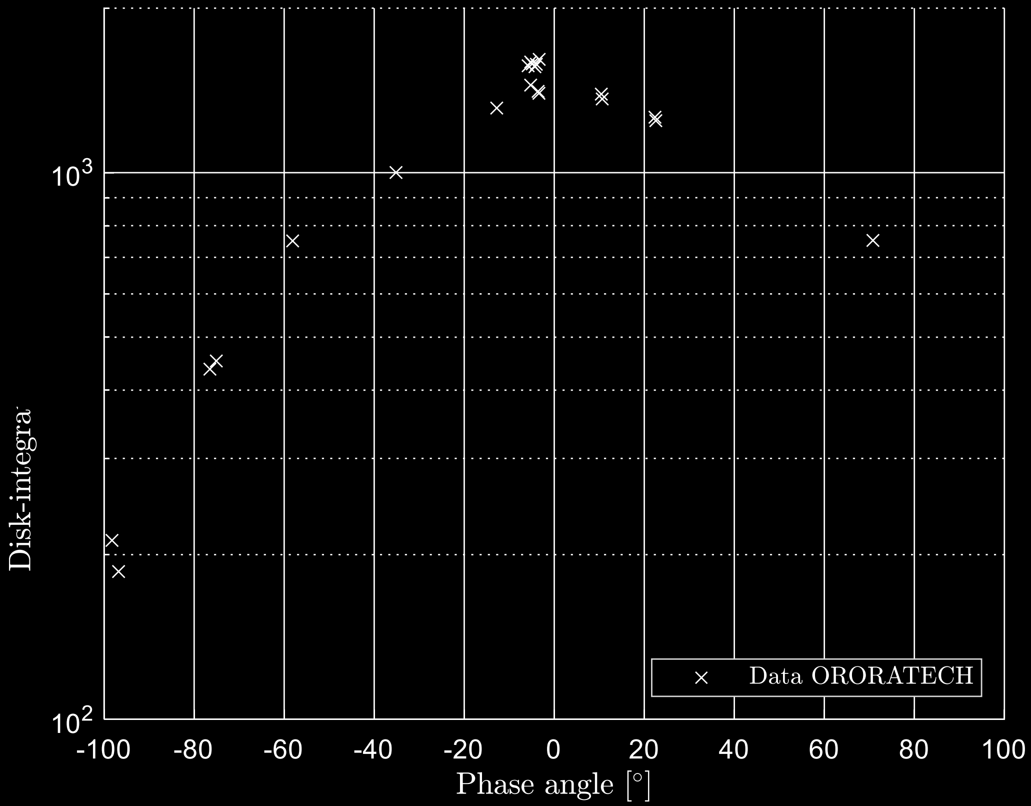

FOREST-2
OroraTech
LWIR band 2
11.4 µm

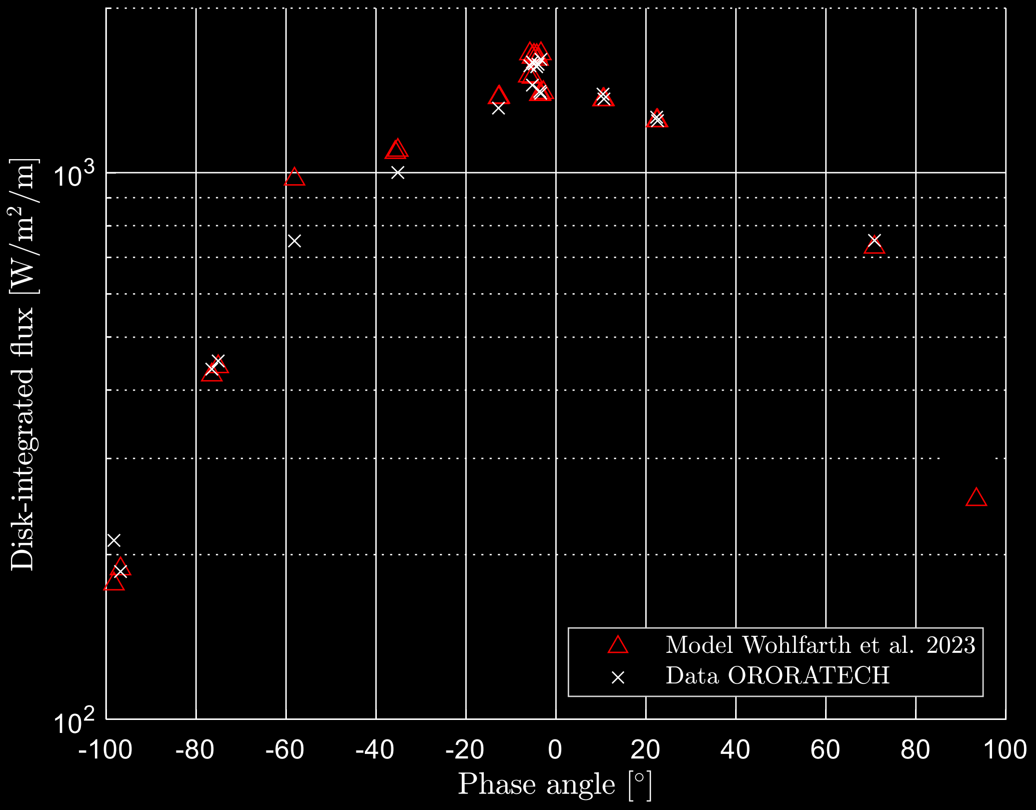

FOREST-2
OroraTech
LWIR band 2
11.4 µm

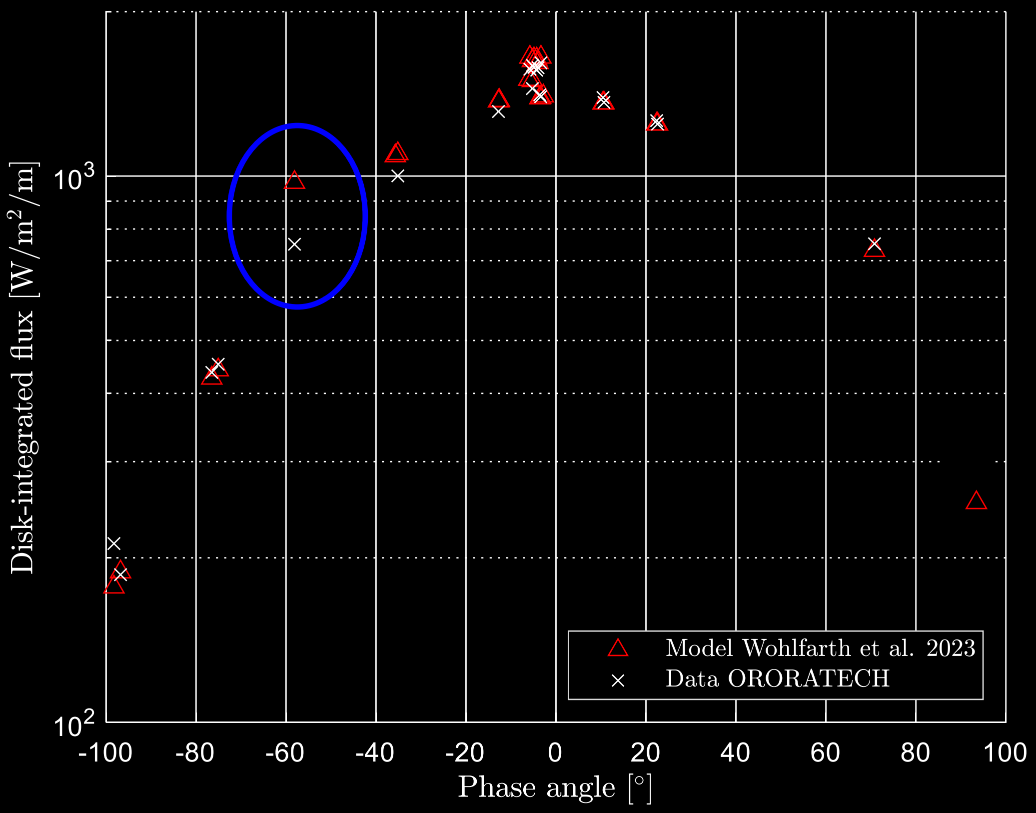

FOREST-2
OroraTech
LWIR band 2
11.4 µm

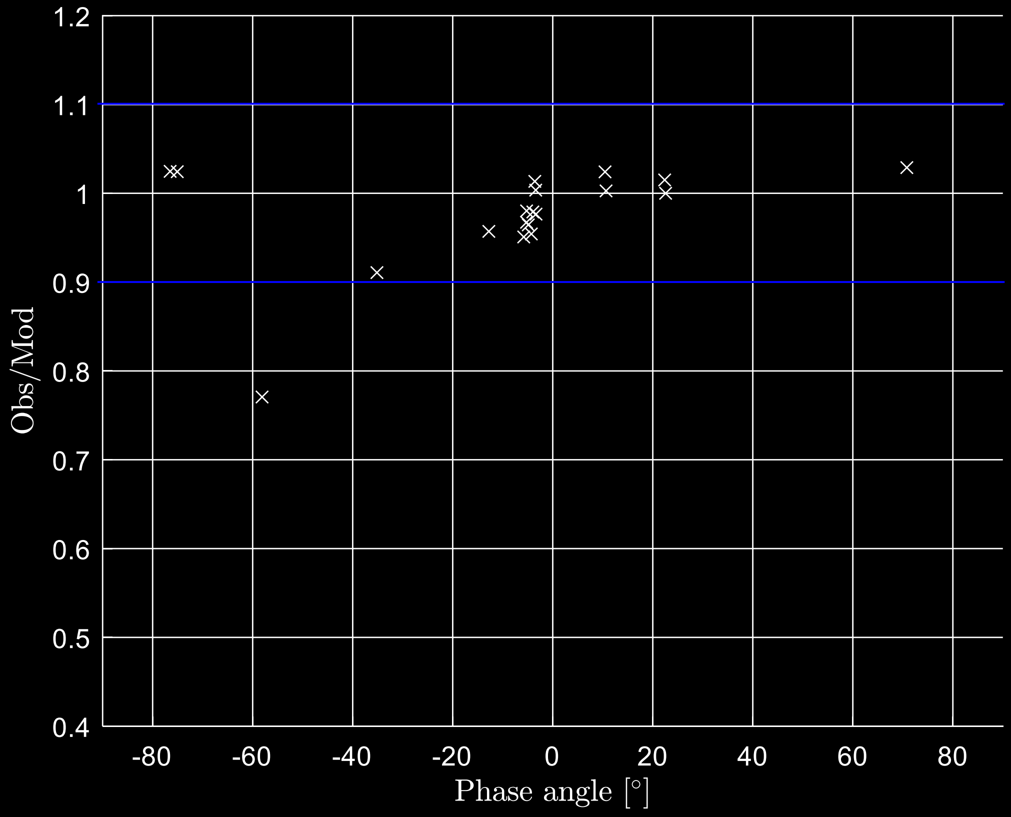

FOREST-2
OroraTech
LWIR band 2
11.4 µm

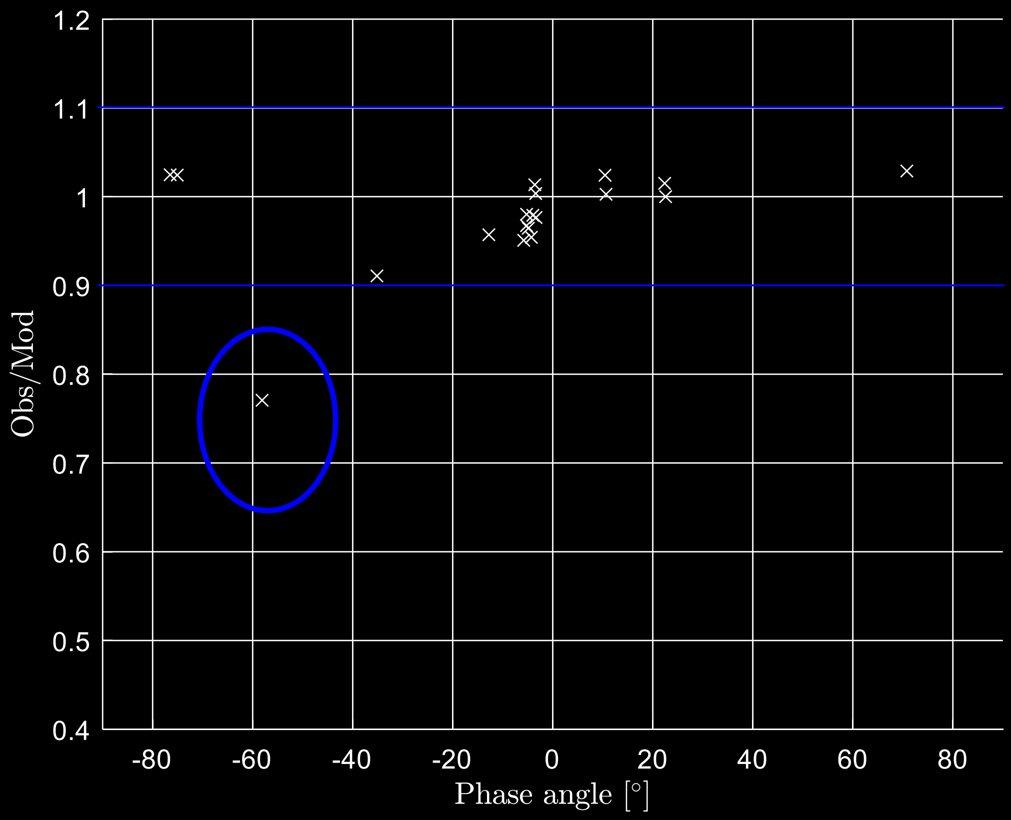

Conclusion

- Successful validation on the Moon (Gaofen-4 in MIR and Diviner in TIR)

- New comparison with HIRS-1/2/3 on NOAA and MetOp
  → excellent agreement, also resembles Müller et al. 2021
- New comparison with ORORATECH Forest-2 L2 (11.4 µm)
  → Good agreement

- More datasets in the future!
- Get the interfacing right for professional use.